

1 **Supporting Information**

2
3 **Ionic liquid-mediated ethosome for transdermal delivery of insulin**

4
5 Fahmida Habib Nabila^a, Rashedul Islam^a, Islam Md Shimul^b, Muhammad Moniruzzaman^c, Rie
6 Wakabayashi^{a,d,e}, Noriho Kamiya^{a,d,e}, Masahiro Goto^{*a,d,e}

7
8 ^aDepartment of Applied Chemistry, Graduate School of Engineering, Kyushu University, 744
9 Motooka, Nishi-ku, Fukuoka 819-0395, Japan

10 ^bDepartment of Nutrition and Food Technology, Jashore University of Science and Technology,
11 Jashore-7408, Bangladesh.

12 ^cChemical Engineering Department, Universiti Teknologi PETRONAS, 32610 Seri Iskandar,
13 Perak, Malaysia

14 ^dAdvanced Transdermal Drug Delivery System Center, Kyushu University, 744 Motooka, Nishi-
15 ku, Fukuoka 819-0395, Japan

16 ^eDivision of Biotechnology, Center for Future Chemistry, Kyushu University, 744 Motooka,
17 Nishi-ku, Fukuoka 819-0395, Japan

18
19 ***Corresponding author**

20 Masahiro Goto, Professor

21 E-mail: m-goto@mail.cstm.kyushu-u.ac.jp.

22 Tel: +81 92 802 2806; Fax: +81 92 802 2810

23

Table of Contents

25	1. Materials and Methods	3
26	1.1. Materials	3
27	1.2. Synthesis of Ionic Liquid	3
28	1.3. Fluorescein Isothiocyanate (FITC) Labeling of Insulin	4
29	1.4. Circular dichroism (CD) spectroscopy	4
30	1.5. Physicochemical characterization and stability study of ETs	4
31	1.6. Entrapment Efficiency of ETs	5
32	1.7. Cell viability assay	6
33	1.8. In Vitro Skin Permeation Study	6
34	1.9. Statistical analysis	7
35	2. Results and discussion	7
36	2.1. FTIR spectra of [EDMPC][Lin], Lin, and DMPC and ¹ H NMR spectra of	
37	[EDMPC][Lin]	7
38	2.2. CD spectra observation	9
39	2.3. MALDI-TOF MS observation of FITC-Insulin	9
40	2.4. Size distribution and Zeta potential of ETs	10
41	2.5. Stability study of ETs	12
42	2.6. Entrapment efficiency of LBIL ETs	12
43	2.7. Drug distribution by CLSM observation	13
44	2.8. Cell viability assay	14
45	2.9. In vitro skin permeation study	15
46	3. References	15

49 **1. Materials and Methods**

50 **1.1. Materials**

51 1,2-Dimyristoyl-*sn*-glycero-3-phosphocholine (DMPC) and ethyl trifluoromethyl sulfonate were
52 purchased from Tokyo Chemical Industry Co. Ltd. (Tokyo, Japan). Linoleic acid (Lin) from
53 Sigma-Aldrich Chemical Co. (St. Louis, MO). Insulin, human, recombinant (Lot. CAM195,
54 potency ≥ 27.5 units/mg), Fluorescein Isothiocyanate Isomer I (FITC-I), D-MEM (Low Glucose)
55 with L-Glutamine and Phenol Red were procured from Wako Pure Chemical Industries Ltd.
56 (Osaka, Japan). Ethanol (99.5%) was purchased from Kishida Chemical Co. Ltd. (Osaka, Japan).
57 PD-10 Sephadex™ G-25 M columns were purchased from Sankei Chemical Co., Ltd.
58 (Kagoshima, Japan)
59 Fetal bovine serum, and antibiotic–antimycotic were purchased from Thermo Fisher Scientific
60 (Waltham, MA, USA). Dulbecco's phosphate buffered saline and trypsin/
61 ethylenediaminetetraacetic acid (0.25% trypsin/1mM ethylenediaminetetraacetic acid) were
62 purchased from Nacalai Tesque (Kyoto, Japan). A WST-8 cell counting kit containing 2-(2-
63 methoxy-4-nitrophenyl)-3-(4-nitrophenyl)-5-(2,4-disulfophenyl)-2H-tetrazolium monosodium
64 salt was purchased from Dojindo Molecular Technologies, Inc. (Kumamoto, Japan). Mammalian
65 cell lines, HeLa were provided by the RIKEN cell bank (Tsukuba, Japan).
66 All the other chemicals and solvents were of analytical grade and used without any further
67 purification.

68 **1.2. Synthesis of ionic liquid**

69 In this experiment, [EDMPC][Lin] consisting of the phospholipid derivative EDMPC as the cation
70 and Lin (18:2) as the anion, was synthesized and characterized following the protocols that were
71 previously reported ¹. The synthesis was confirmed by Fourier transform infrared (FTIR)
72 spectroscopy (Fig. S1). The FTIR spectra of synthesized LBILs were recorded by a Perkin Elmer
73 FTIR spectrophotometer with a diamond crystal reflection sampler. All samples were analyzed in
74 the range of 400 – 4000 cm^{-1} with 20 scans accumulation. Spectral outputs were recorded in a
75 transmittance mode as a function of wave number. ¹H-NMR of [EDMPC][Lin] was employed by
76 dissolving it in the chloroform-d solution. Spectrum data were processed by the Delta-V software
77 package (version 5.0.5.1, JEOL) where coupling constants (J) were in Hz units.

78 **1.3. Fluorescein isothiocyanate (FITC) labeling of insulin**

79 FITC labeling of Insulin was prepared following a previously reported protocol ³ with a minor
80 modification. Briefly, Human-derived Insulin was dissolved in 0.1M HCl, and 0.1M Sodium
81 Bicarbonate buffer (P^H 9.3) was added to create a 10mg/mL insulin solution. FITC was dissolved
82 in DMSO to create a 5mg/mL solution, and both solutions were gently mixed with a molar ratio
83 of FITC:insulin 3:1 while shielded from light for 2.5 hours at room temperature (RT) with gentle
84 continuing stirring. The resulting FITC-labeled Insulin (FITC-Insulin) mixture was collected using
85 a PD-10 SephadexTM G-25 column and subsequently freeze-dried to obtain the final powdered
86 form of FITC-Ins. The quality of FITC-Ins was confirmed through Matrix-assisted laser
87 desorption/ionization-time of flight (MALDI-TOF) mass spectrometry (MS) (Fig. S4).

88 **1.4. Circular dichroism (CD) spectroscopy**

89 CD spectroscopy was employed to assess the stability of insulin's secondary structure in both 20-
90 40% ethanol and 25-35% ETs. The J-1500 CD spectrometer (JASCO, Tokyo, Japan) was utilized
91 with the parameters presented in Table S1.

92

93

Table S1. Parameters for CD measurement

Cell	Path length (mm)	Wavelength range (nm)	Integral count	Temperature (°C)
Quartz cell	0.1mm	190 - 250	5	25

94 The obtained CD spectra were subjected to an adaptive smoothing method and then converted to
95 the absolute value of CD.

96 **1.5. Physicochemical characterization and stability study of ETs**

97 **1.5.1. Particle size and zeta potential (ZP/ ζ) distribution**

98 Particle size and ZP distribution were determined using a Zetasizer Nano ZSP (Malvern, Nano
99 series, Worcestershire, WR14 1XZ, U.K.) through dynamic light scattering (DLS) measurements.
100 These measurements aimed to calculate the average hydrodynamic radius (R_H) and ZP, ζ of the
101 particles. Disposable cuvettes were positioned at an angle of 173°, and the temperature was
102 maintained at 25 ± 0.1°C during the measurements. Five measurements were taken for each
103 sample, and the mean values were calculated using the Zetasizer 7.03 software, which provided

104 Z-averaged values of R_H and polydispersity index (PDI). The R_H calculation was conducted by the
105 Stokes-Einstein equation,

$$106 \quad D = \frac{kT}{6\pi\eta R_H^4}$$

107 Here, D represents the translational diffusion coefficient, k is the Boltzmann's constant, T is the
108 absolute temperature, and η is the solvent viscosity. ZP, ζ was calculated by the measurement of
109 the electrophoretic mobility using the Hemholtz-Smoluchowski equation.⁵ Stability assessments
110 of the formulations were performed at different time points over a period of 12 weeks.

111 **1.5.2. Morphology of ETs by TEM & CLSM**

112 A JEOL JEM-2010 Transmission Electron Microscopy (TEM) was employed to examine the size
113 and shape of the ETs. Sample preparation involved placing 5 μ L aliquots on a carbon film-coated
114 copper grid, allowing them to air-dry for 2 minutes (min), and removing excess material with filter
115 paper. Staining was performed by applying 2.5 μ L of 2% uranyl acetate solution, followed by a 5
116 min incubation. Subsequently, the TEM grid was vacuum-dried in a desiccator, and TEM images
117 were captured at an accelerating voltage of 120 kV.

118 For confocal laser scanning microscope (CLSM) examination, a 5 μ L formulation was mounted
119 between a glass slide and a cover glass for fixation. The observation was made using a Carl Zeiss
120 LSM700 microscope, Oberkochen, Germany at 63X magnification. Image processing was
121 performed using LSM software from Carl Zeiss

122 **1.6. Entrapment efficiency of ETs**

123 The Encapsulation efficiency (%EE) was determined through fluorescence spectrophotometry.
124 Non-encapsulated drug quantification was determined using a centrifuge concentrator method:
125 Formulations were centrifuged using the TOMY MX-307, HIGH SPEED REFRIGERATED
126 MICRO CENTRIFUGE, at 14,000 rpm at 4 °C for 30 min. The resulting supernatant was
127 transferred to a separate Eppendorf tube and subjected to a secondary centrifugation for 15 min at
128 14,000 rpm.

129 The total quantity of unentrapped FITC-Insulin was assessed using a microplate spectrophotometer
130 (Bio-Rad, Tokyo, Japan) within the wavelength range of 485 to 535 nm. Each sample underwent
131 three evaluations.^{6,7}

132 The percentage of encapsulated drug amount was calculated using the following formula:

$$133 \text{ EE (\%)} = \frac{\text{Amount of drug used} - \text{uncapsulated drug}}{\text{Total amount of drug}} \times 100$$

134 **1.7. Cell viability assay**

135 The WST-8 cell viability assay was conducted using HeLa mammalian cell lines following a
136 protocol outlined in the literature with some modifications.⁸ HeLa cells were cultured until they
137 reached approximately 70-80% confluency and were harvested from the cell culture dish through
138 trypsinization. Subsequently, the cells were seeded into 96-well flat-bottomed plates at a density
139 of 1.5×10^4 cells per well (100 μL , concentration: 1.5×10^4 cells per mL) and cultured in MEM
140 (containing 10% fetal bovine serum and 1% antibiotic-antimycotic) for 24 hours at 37°C in a CO₂
141 incubator.

142 Next, 2 μL of ET1, ET2, ET3, and ET4 formulations were added to the respective wells.
143 Dulbecco's Phosphate-Buffered Saline (D-PBS), 25% ethanol (E25), and 1 mg/mL insulin solution
144 were used as positive controls, while 5% Sodium Dodecyl Sulfate (SDS) was used as the negative
145 control. The cells were further incubated for 24 hours. Subsequently, 10 μL of the Cell Counting
146 Kit-8 solution was added and incubated for 3 hours to initiate the color reaction. The absorbance
147 was measured at 450nm using a microplate spectrophotometer (Bio-Rad, Tokyo, Japan). As a
148 negative control, 10 μL of the WST-8 solution was added, and for the blank, 10 μL of MEM
149 medium was added instead of the WST-8 solution to the wells. Cell viability was calculated using
150 the following formula:

$$151 \text{ Cell viability [\%]} = [(A_s - A_b) / (A_c - A_b)] \times 100$$

152 Where: A_s = Absorbance of the sample; A_c = Negative control absorbance; A_b = Blank absorbance.

153 **1.8. *In vitro* skin permeation study**

154 Mouse skin penetration was evaluated for various formulations loaded with FITC-Insulin using a
155 Franz diffusion cell (FDC) following a previously established procedure.⁹ Mouse skin sections
156 (Hos: HR-1) were purchased from Hoshino Laboratory Animals (Ibaraki, Japan) and stored at -

157 80°C. Skin sections were dissected into 2 cm × 2 cm square pieces with a scalpel for the *in vitro*
158 experiment. In the FDC setup, the receiver phase contained 4 mL of 1X PBS buffer and was
159 equipped with a magnetic stirrer. Mouse skin pieces were affixed to the upper side of the receiver
160 phase, with the stratum corneum (SC) facing outward, serving as the donor compartment. To
161 eliminate air bubbles, 1 mL of PBS buffer was introduced through the branch tube into the FDC.
162 FITC-Insulin formulations (1mg/mL) with varying compositions were applied in 200µL onto the
163 mouse skin within the donor compartment. After a 6-hour incubation, 1mL samples were collected
164 from the receiver phase of all FDCs using syringes.
165 To quantify the topically delivered drug amount, the skin was unclamped, cleansed with Milli-Q
166 water and 20% ethanol, and then sectioned into >16 slices using a scalpel. The skin slices were
167 immersed in an extraction solution comprising PBS-ACN-MeOH (2:1:1; v/v/v) at RT for 12 hours
168 (Fig. 4(b)) and 15 hours (Fig. 4(d)) with continuous agitation. The insulin content in the collected
169 samples was assessed using a microplate spectrophotometer (iMARK, Bio-Rad, Tokyo, Japan).

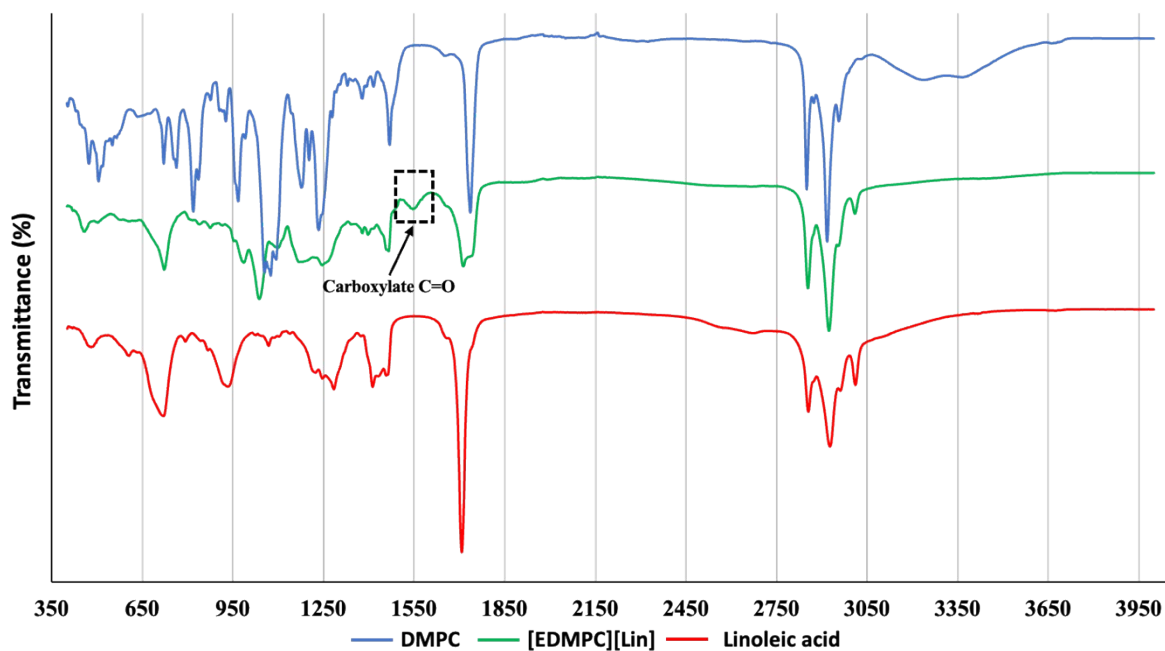
170 **1.9. Statistical analysis**

171 Statistical analysis was performed using GraphPad Prism software (Version 6.05). One-way
172 ANOVA with Dunnett's Multiple Comparison test was used to determine the statistical
173 significance of the data. A *P*-value < 0.05 was considered statistically significant. All values shown
174 here were carried out as the mean ± standard deviation.

175 **2. Results and discussion**

176 **2.1. FTIR spectra of [EDMPC][Lin], Lin and DMPC and ¹H-NMR spectra of** 177 **[EDMPC][Lin]**

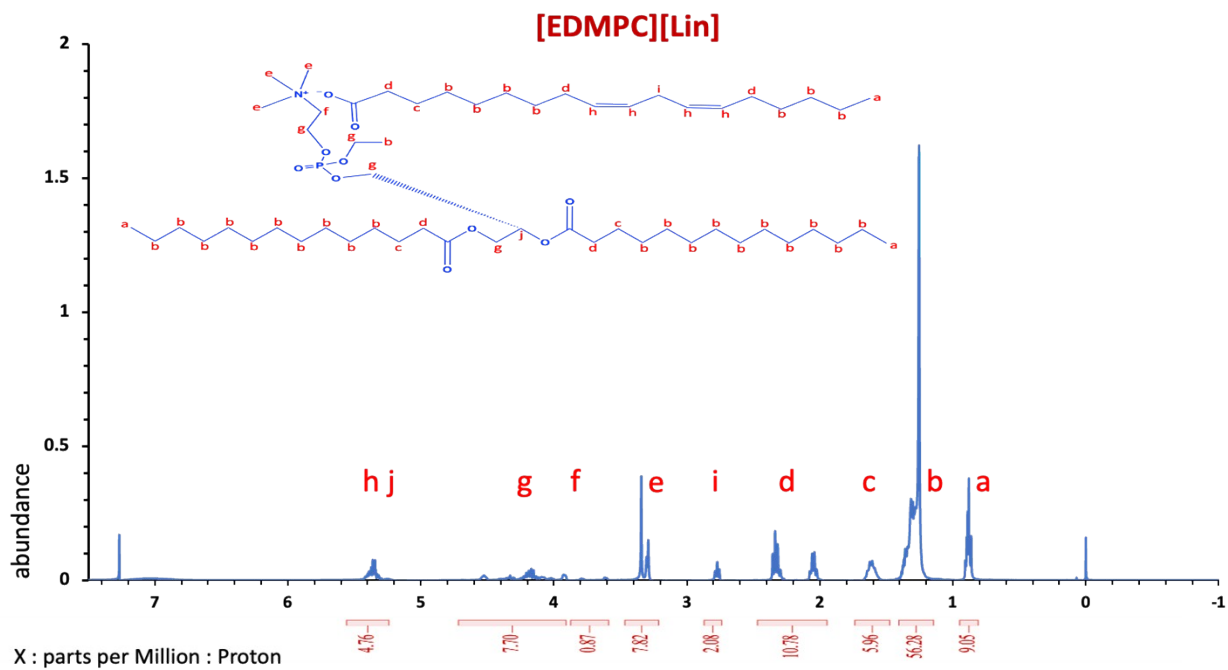
178 The FTIR spectra of [EDMPC][Lin], Lin, and DMPC were analyzed to confirm the synthesis of
179 IL. The distinctive C=O stretching peak from carboxylate of the synthesized [EDMPC][Lin] was
180 observed in the region of 1545 cm⁻¹. The detailed FTIR analysis along with the ¹H NMR findings
181 indicates the successful synthesis of [EDMPC][Lin] (Fig. S1 and Fig. S2).



182

183

Fig. S1 FTIR-spectra of [EDMPC][Lin], Lin, and DMPC

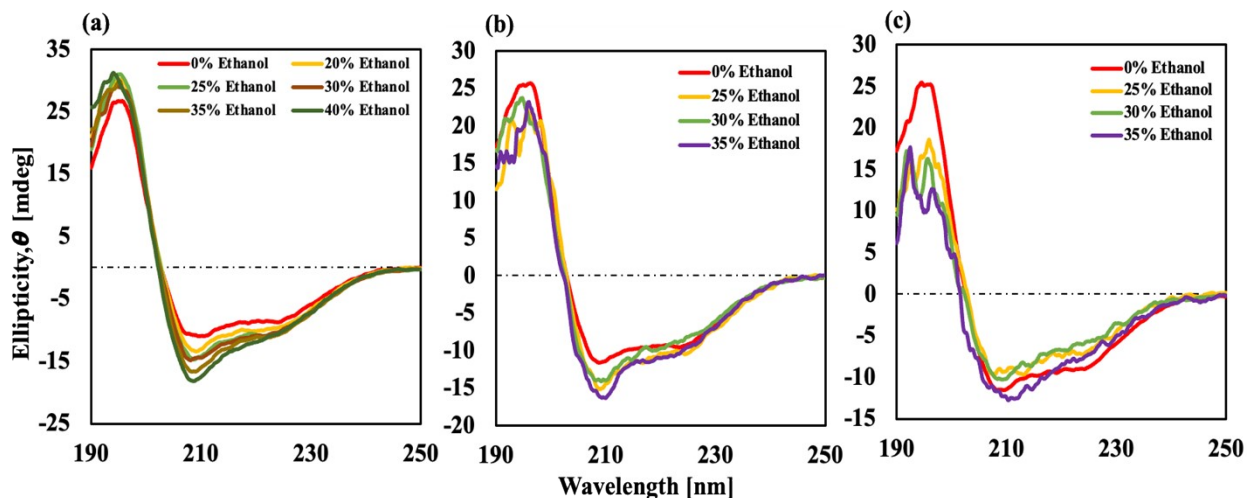


184

185

Fig. S2 ^1H -NMR spectra of [EDMPC][Lin]

186 **2.2. CD spectra observation**

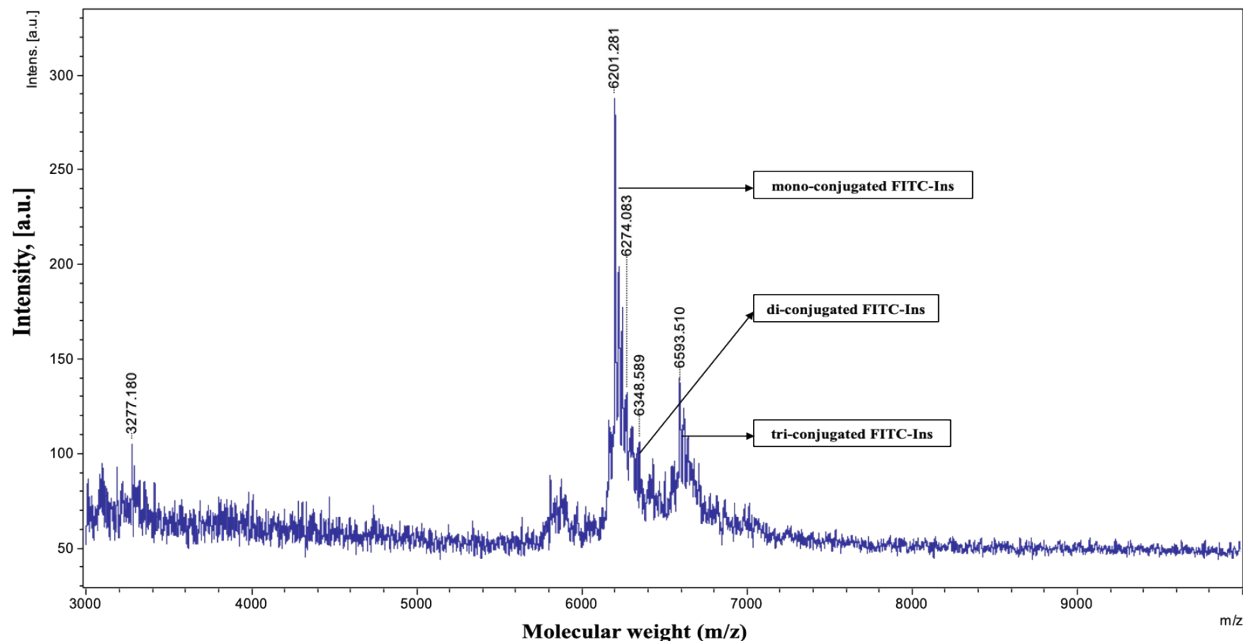


187

188 **Fig. S3** CD spectra showing the conformational change of insulin in (a) 20-40% ethanol; ETs (b)
189 after sonication, and (c) after homogenization in 25-35% ethanol

190 **2.3. MALDI-TOF MS observation of FITC-Insulin**

191 The MALDI-TOF MS analysis of FITC-Insulin revealed a notably high-intensity peak for the
192 mono-conjugate of FITC-Insulin, with very minor peaks for di and tri-conjugated FITC-Insulin
193 (Fig. S4).



194

195

Fig. S4 MALDI-TOF MS spectrum of FITC-Insulin

196 **2.4. Size distribution and ZP of ETs**

197 ETs were prepared using DMPC and [EDMPC][Lin] with and without any drugs to assess
198 successful vesicle preparation in the presence of ethanol. ETs were successfully synthesized using
199 both DMPC and [EDMPC][Lin].

200

201 **Table S2.** Composition of LBIL ethosomal systems.

Samples	[EDMPC][Lin] (mM)	DMPC (mM)	Ethanol (w/w%)	Water (w/w%)
ET1	5	-	25.35	75.65
ET2	10	-	25.35	75.65
ET3	15	-	25.35	75.65
ET4	20	-	25.35	75.65
ET5	-	10	25.35	75.65
ET5	-	20	25.35	75.65

202 The size distribution of [EDMPC][Lin] and DMPC-mediated ETs without insulin was observed,
203 revealing that the [EDMPC][Lin] ETs exhibited a larger vesicle size compared to that of DMPC
204 ETs (**Table S3.**).

205

206 **Table S3.** Size distribution and ZP of ETs without drug

System	Z-Ave(nm)	PDI	ZP (mV)
ET2	377.3 ± 9.479	0.126 ± 0.043	45.9±2.68
ET4	374.1 ± 6.016	0.130 ± 0.047	53.8±2.51
ET5	230.0 ± 3.680	0.105 ± 0.058	-11.3±0.624
ET6	246.2 ± 5.658	0.134 ± 0.063	-8.66±0.499

207

208 **2.4.1. FITC-Insulin loaded ETs**

209 After loading with the FITC-Insulin drug, the DMPC ETs exhibited instability, characterized by
210 significant variability in size and elevated PDI values (**Table S3.**). Within 24 hours, it became
211 totally unstable to measure the DLS readings.

212

213 **Table S4.** Size distribution of DMPC-mediated ETs loaded with FITC-Insulin

System	Z-Avg (nm)	PDI
ET5	4678±442	0.584±0.332
ET6	4863±1359	0.714±0.330

214 With the loading of the FITC-Insulin drug the [EDMPC][Lin] ETs were stable with an increase in
215 size.

216

217 **Table S5.** [EDMPC][Lin] ETs Z-Average and PDI values after loading with FITC-Insulin.

System	Z-Avg (nm)	PDI
ET2	604.2±34.9	0.324±0.054
ET4	609.8±47.2	0.402±0.130

218 **2.4.2. Size reduction of ET formulations**

219 The size distribution of nanovesicles is a critical factor in achieving effective drug delivery ¹⁰. In
220 our study, we utilized a combination of probe sonication and homogenization techniques to
221 systematically reduce the size of 10mM [EDMPC][Lin] ETs at varying ethanol concentrations.
222 Specifically, the application of a sonicator led to successful and uniform size reduction.

223

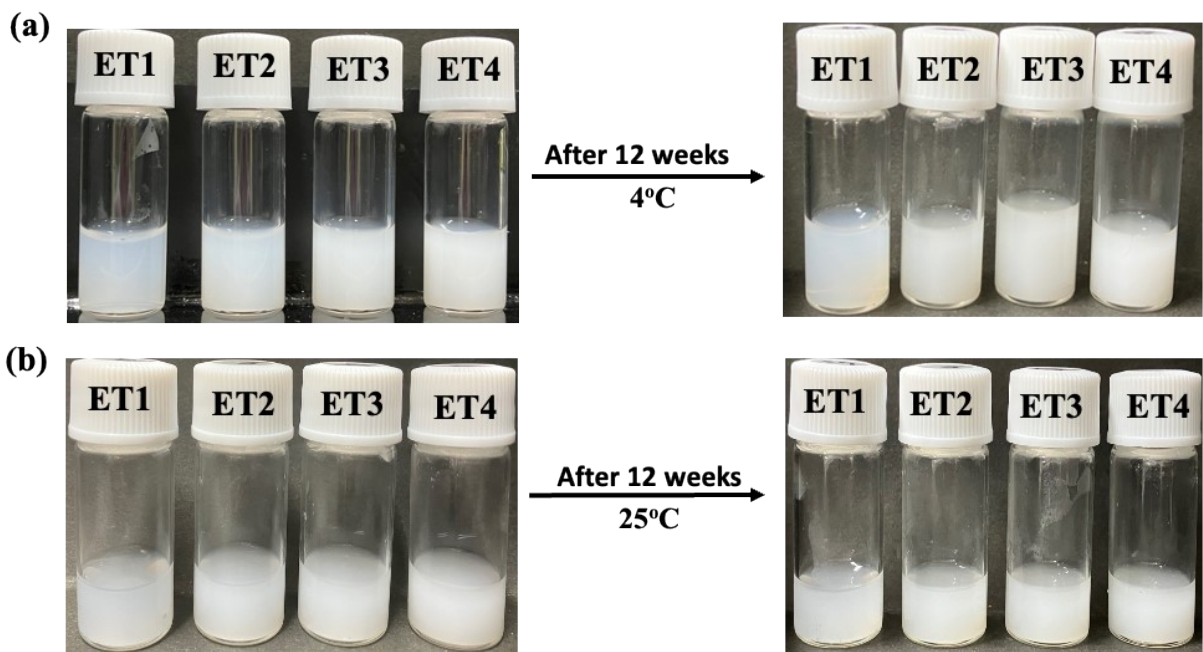
224 **Table S6.** Z-average and PDI values for ET2 formulation

Ethanol conc. (vol/vol)	Sonicator		Homogenizer	
	Z-Avg (nm)	PDI	Z-Avg (nm)	PDI
35%	384.23±6.04	0.255±0.03	683.53±23.95	0.349±0.06

225

226

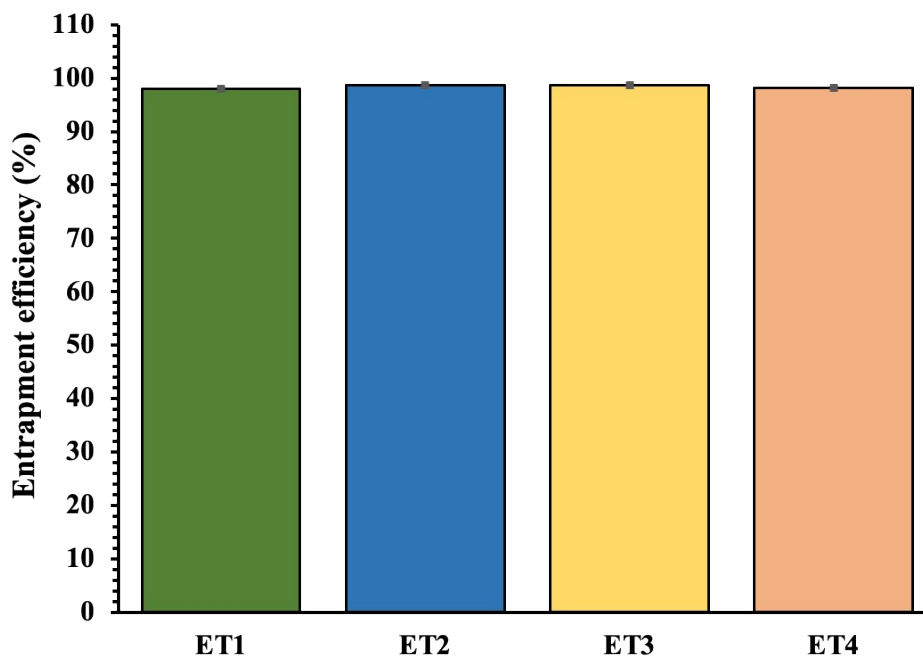
227 2.5. Stability study of ETs



228

229 Fig. S5 Physical appearances of LBIL ETs before and after 12 weeks; (a) at 4°C; (b) at 25°C.

230 2.6. Entrapment efficiency of LBIL ETs

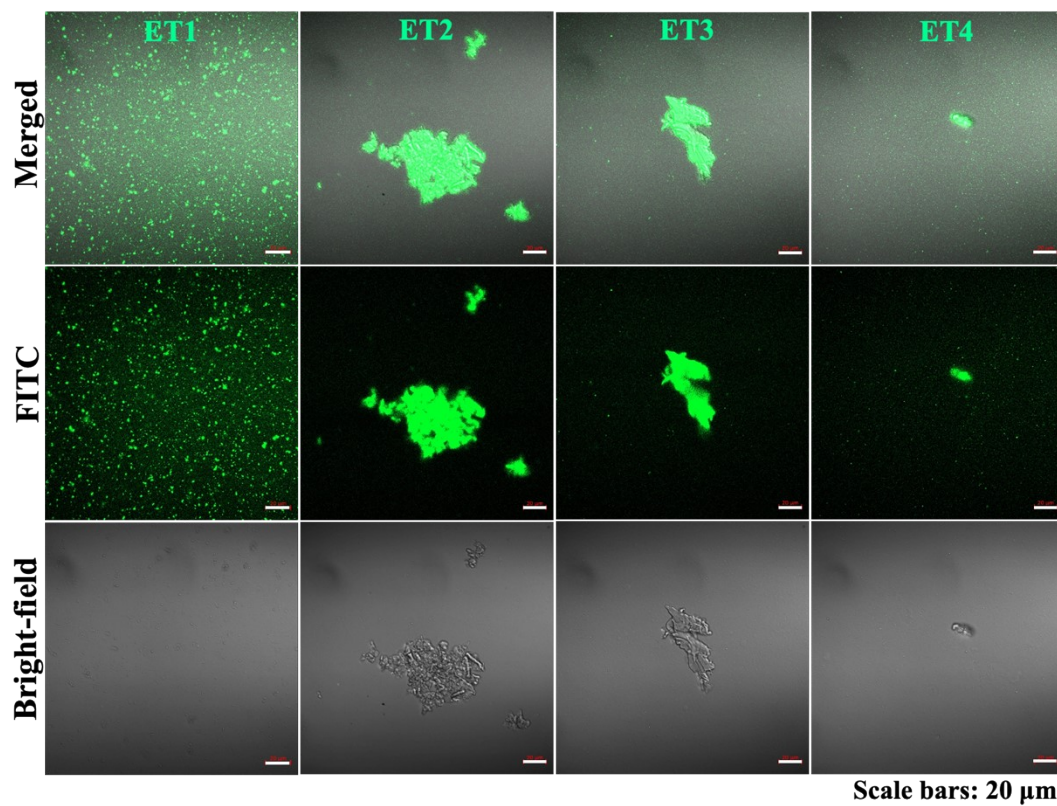


231

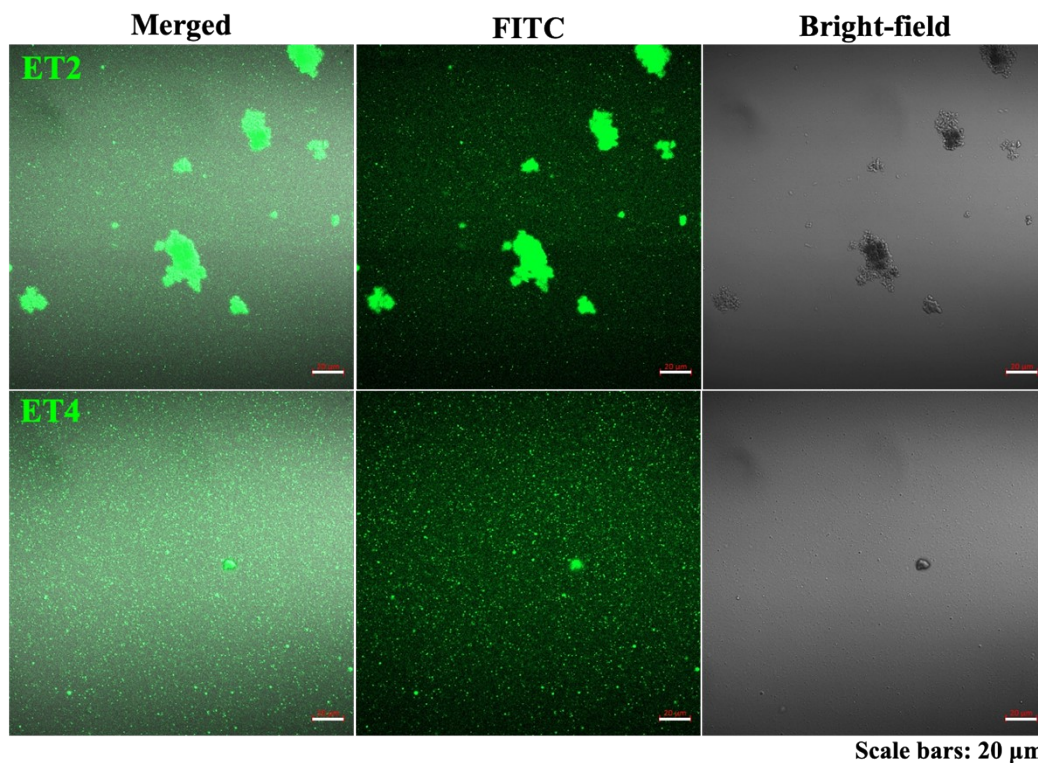
232

233 Fig. S6 Percent entrapment efficiency of ET formulations. All the data represent the average of
234 the three experiments, and the error bars indicate the standard deviation.

235 2.7. Drug distribution by CLSM observation

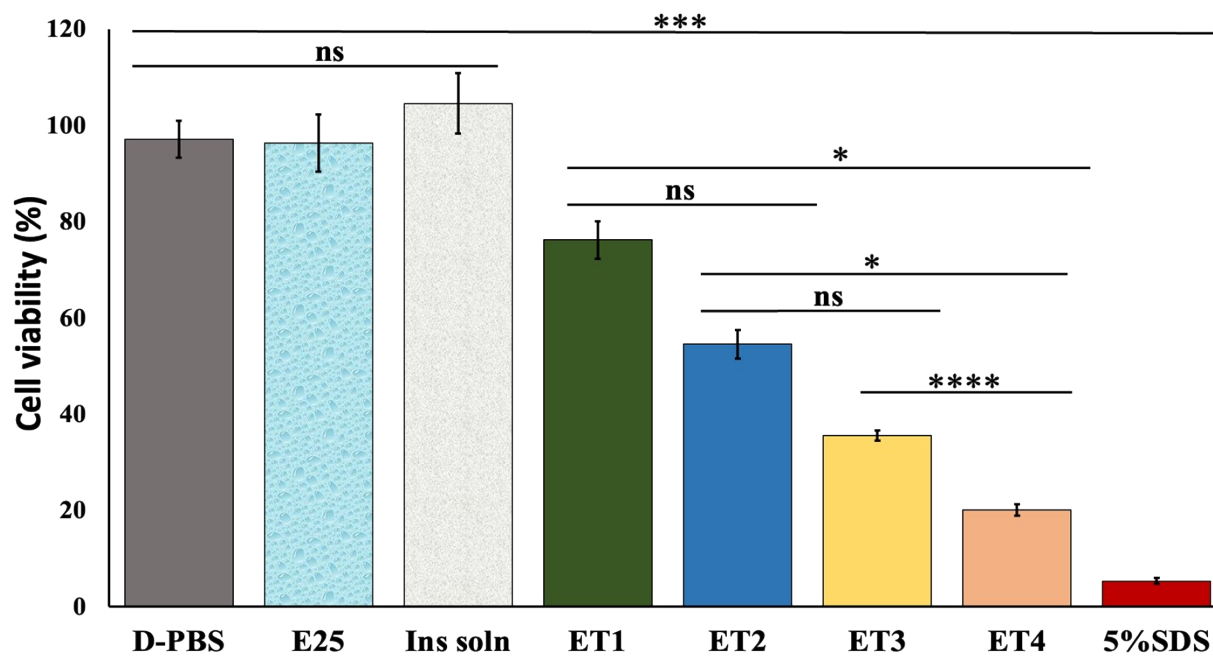


236
237 **Fig. S7** Drug distribution observation of ET1, ET2, ET3 & ET4 encapsulated with FITC-Insulin
238 by CLSM visualization through a 63X lens.



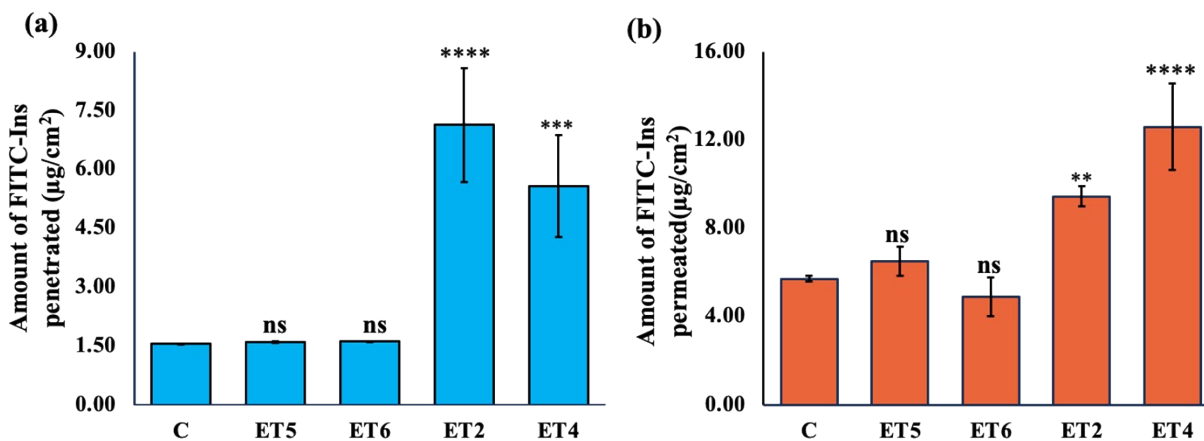
239
 240 **Fig. S8** Drug distribution observation of ET2 and ET4 prepared with 35% ethanol encapsulated
 241 with FITC-Insulin by CLSM visualization through a 63X lens.

242 **2.8. Cell viability assay**



243
 244 **Fig. S9** Cytotoxicity of IL ETs towards HeLa cell lines, N = 10; mean \pm SD; ns means,
 245 nonsignificant, *, $P < 0.05$; ***, $P < 0.001$; ****, $P < 0.0001$ (Tukey multiple comparison test)

246 **2.9. In vitro skin permeation study**



247

248 **Fig. S10** In vitro skin permeation study, (a) drug penetration and (b) drug permeation by ETs in
 249 mouse skin. Here, C, control FITC-insulin solution (1mg/mL); ns, non-significant; * $p < 0.05$, **
 250 $p < 0.005$, *** $p < 0.001$, **** $p < 0.0001$ (Dunnett's multiple comparison test).
 251

252 **3. References**

- 253 1 S. Uddin, M. R. Chowdhury, R. Wakabayashi, N. Kamiya, M. Moniruzzaman and M.
 254 Goto, *Chem. Comm.*, 2020, **56**, 13756–13759.
- 255 2 R. C. MacDonald, V. A. Rakhmanova, K. L. Choi, H. S. Rosenzweig and M. K. Lahiri,
 256 *J Pharm Sci*, 1999, **88**, 896–904.
- 257 3 D. Shah, Y. Guo, J. Ocando and J. Shao, *J Pharm Anal*, 2019, **9**, 400–405.
- 258 4 D. A. Kuznetsova, E. A. Vasilieva, D. M. Kuznetsov, O. A. Lenina, S. K. Filippov, K. A.
 259 Petrov, L. Y. Zakharova and O. G. Sinyashin, *ACS Omega*, 2022, **7**, 25741–25750.
- 260 5 A. Sze, D. Erickson, L. Ren and D. Li, *J Colloid Interface Sci*, 2003, **261**, 402–410.
- 261 6 P. P. Shah, P. R. Desai and M. Singh, *J. Control. Rel.*, 2012, **158**, 336–345.
- 262 7 S. Paliwal, A. Tilak, J. Sharma, V. Dave, S. Sharma, R. Yadav, S. Patel, K. Verma and K.
 263 Tak, *Lipids Health Dis*, 2019, **18**, 1–15.
- 264 8 R. M. Moshikur, M. R. Chowdhury, R. Wakabayashi, Y. Tahara, M. Moniruzzaman and
 265 M. Goto, *Int J Pharm*, 2018, **546**, 31–38.
- 266 9 M. R. Islam, S. Uddin, M. R. Chowdhury, R. Wakabayashi, M. Moniruzzaman and M.
 267 Goto, *ACS Appl. Mat. Inter.*, 2021, **13**, 42461–42472.
- 268 10 A. Laouini, C. Jaafar-Maalej, I. Limayem-Blouza, S. Sfar, C. Charcosset and H. Fessi,
 269 *J Colloid Sci. and Biotech.*, 2012, **1**, 147–168.
 270